J. Fac. Cul. Edu. Saga Univ.
Vol. 1, No. 1 (1997) 343～357

Computational Study on the Reaction Paths of [2,3]-Wittig Rearrangement

Toshiya OKAJIMA

Abstract

The transition structures of [2,3]-Wittig rearrangement have been studied, by use of *ab initio* molecular orbital method. Energies of all stationary points, including reactants, transition structures, intermediates, and products, located at the 3-21G basis set, were evaluated at the second order Moller-Plesset correlation level with the 6-31(+)G(*) basis sets. The reaction paths, obtained by intrinsic reaction coordinate (IRC) calculation, were also analyzed.

Introduction

The [2,3] sigmatropic rearrangement[1] has been an efficient method for acyclic stereocontrol.[2,3] The rearrangement involving an α-oxycarbanion as the migrating terminus ([2,3]-Wittig rearrangement, Figure 1 (eq.1)) allows the regio- and stereoselective substitution of the hydroxyl group of an homoallylic alcohol with a functionalized carbon moiety.[4,5] The attention has focused on the stereochemistry of the migrating termini (vicinal chiral centers) as well as the olefin geometry. Substitution pattern at the anion center as well as on the allylic ether can have profound effects on the stereochemistry of the rearranged product. However, it has not been clear what effect would be exhibited by the parent anion for the conformational preference of transition-state structure and the

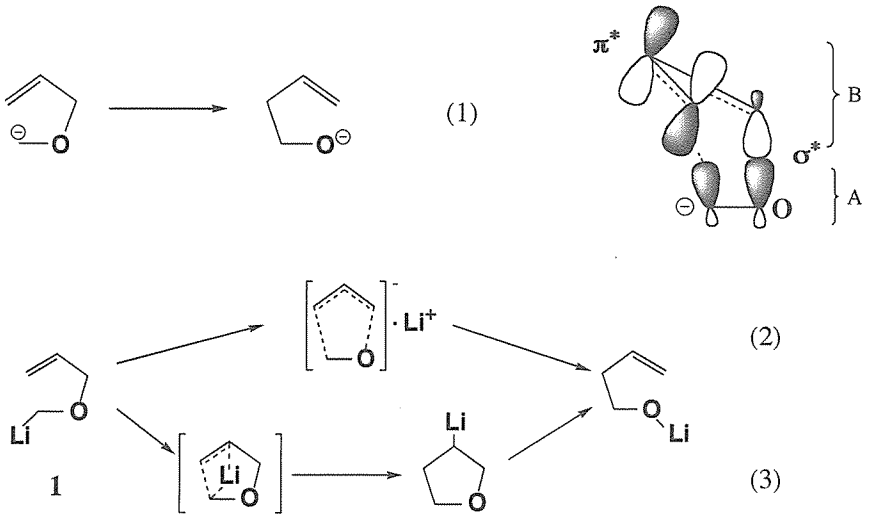

Figure 1. Plausible mechanisms (concerted (eq.(2)) and stepwise (eq.(3))) for [2,3]-Wittig rearrangement (eq.(1)).

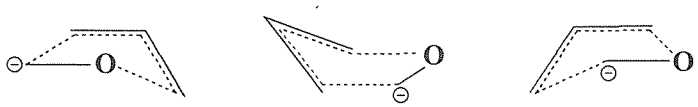

I II III

Figure 2. Three transition-state models (Trost's type (**I**), Rautenstrach's type (**II**), and Nakai's type (**III**) for [2,3]-Wittig rearrangement.

mechanism of this rearrangement is also not fully understood. It is extremely important to understand factors determining the transition-state structures, though three conceptual models of transition -state geometry have been suggested so far. Because of the synthetic potential of this transformations, the author have explored the nature of this rearrangement of parent lithiomethyl vinyl ether (**1**), along with the non-lithiated species,[6] expecting that the results may serve as a guiding principle for designing highly stereospecific [2,3]-Wittig modifications.

[2,3]-Wittig rearrangement can be defined as a thermal isomerization that proceeds through a six-electron, highly ordered cyclic transition state to create both a new C-C double bond and a new C-C single bond accompanied with C-O bond breaking (concerted process), as shown in eq.(2) in Figure 1.[7] In order to explain the stereochemistry of the [2,3]-Wittig rearrangement, three basic conformation for the five-membered "folded-envelop" transition states have been suggested, which are shown in Figure 2. Conformer **I** has been used for the ylide [2,3]-processes[8] and conformer **II**, which originally proposed by Rautenstrach, has been most frequently assumed.[9] Most recently, conformer **III** has been proposed by Nakai et al.[10] Although the concerted transition states with envelop conformations have been assumed to be involved in the reaction, there still remains another path (stepwise process), as depicted in eq.(3) in Figure 1.[11]

Calculational Method

Molecular orbital (MO) calculations were performed by using GAUSSIAN 94 quantum chemical program packages for *ab initio*[12] SCF-MO calculations developed by Pople and co-workers, on the Power Indigo2 work station of the Information Processing Center of Saga University. Geometries of stationary points were fully optimized without symmetry constrainst at the single determinantal Hartree-Fock level of MO theory, using the gradient techniques at the split valence 3-21G basis set.[13] All ground states and transition structures are characterized by diagonalization of the force constant matrix. (minima and first order saddle-points, the latter having only one negative imaginary vibrational frequency corresponding to motion along the reaction coordinate) A general procedure for locating transition structures involves stepping along the reaction vector (the vibrational mode with the negative eigenvalue in the Hessian matrix) and terminating the procedure at the geometry when the stationary point is met.[14] It is known that 3-21G basis set generally gives reliable results on geometries. In the notation of the basis set used, the symbol "*" designates the basis set including polarization functions and "+" diffusion functions on heavy atoms except hydrogen. The energy barriers for the reaction were computed as the difference in SCF energy between stationary points. Since it is known that large superposition errors (BSSE) occur with the small 3-21G basis set, the

energy calculations were also performed at more sophisticated levels.[15] Electron correlation was considered using Moller-Plesset perturbation theory[16] truncated to the second order (MP2[17]) by calculating single point energies[18] using HF wave functions computed at 3-21G optimized geometries with the 6-31(+)G(*) basis sets for generating electronic configurations. Only excitations of valence electrons were included in the correlation expansion (frozen-core approximation).[19] The energies were calculated at several levels of theory to ensure the accuracy of the geometries and energetic. We have followed Pople's conventions for shorthand notations for describing the level of a calculation. The level of theory is followed by a slash and then the basis set description. Single point calculations are designated with the energy first and the level of the geometry optimization second. For example, MP2/6-31G(FC)//RHF/3-21G signifies a single point frozen core MP2 calculation with 6-31G basis set at RHF/3-21G optimized geometry. The mass-weighted minimum energy path (the intrinsic reaction coordinate (IRC)) calculations at the 3-21G level on all transition structures were followed from the transition structures to the local minima, using the steepest descent algorithm (in mass-weighted Cartesian coordinates). Enough numbers of points to identify the minima, linked with transition structures, were optimized stepping into the direction of both the reactant and product side. The naming of "transition structure" (the saddle point on a potential energy surface) rather than "transition state" (free energy maximum) is used in this context.[20] "**TS**" is an abbreviation for "transition structure" and "**INT**" for "five-melbered intermediate". Since, the rearrangement was generally performed in tetrahydrofuran (THF) by using alkyllithium reagents as the base at low temperatures, Li has been chosen as the metal cation in this study.

Geometries

First of all, The author has performed *ab initio* calculation for [2,3]-Wittig rearrangement of non-lithiated **1**. Only one transition structure (non-lithiated **TS-I**) could be located at the 3-21G basis set, which is shown in Figure 3. The transition structure for the non-lithiated **1** has forming C_1-C_5

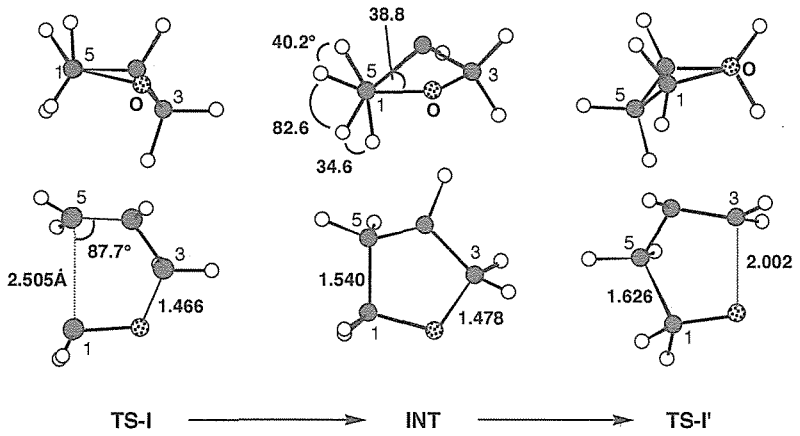

Figure 3. 3-21G transition structures (Trost's type (**TS-I** for C-C bond forming and **TS-I'** for C-O bond breaking step) and the intermediate (**INT**) for [2,3]-Wittig rearrangement of non-lithiated **1**.

bond lengths of 2.505Å, indicating that the C_1-C_5 bond is formed to a large extent, though the O_2-C_3 bond is only slightly broken (1.466Å). Since C_5 atom is slightly pyramidalized at transition state, the transition state can be referred to be quite early. As described below, IRC calculation for [2,3]-Wittig rearrangement of **1** reveals that non-lithiated **TS-I** corresponds to the stepwise process, leading to the five membered ring intermediate (**INT**). That is, non-lithiated **TS-I** corresponds to C_1-C_5 bond forming TS. **TS-I** has fundamentally Trost's type envelop (**I**), which has the long distance (2.505Å) between C_1 and C_5 atom and almost eclipsed conformation around the forming C_1-C_5 bond. However, the dihedral angle (O_2-C_1. . . C_5-C_4) is considerably large (12.7°, which value is exactly 0° for Trost's envelop **I** in Figure 2). In the intermediate (**INT**), having complete C_1-C_5 single bond (1.540Å), the conformation around C_1-C_5 bond was changed to almost staggered (each dihedral angle is 40.2, 86.2, and 34.6°, respectively (Figure 3)) and the dihedral angle of O_2-C_1-C_5-C_4 is also large (38.8°). In O_2-C_3 bond breaking **TS-I'** leading to the final alcoholic product (Figure 3), breaking O_2-C_3 bond length is 2.002Å. In this TS, C_1-C_5 bond is slightly elongated (1.626Å) as compared to that (1.540Å) of **INT**. In **TS-I'**, the dihedral angle C_1-O_2..C_3-C_4 is only 15.0°. Thus, without consideration of metal cation (Li^+), only one route proceeding through **TS-I**, having fundamentally Trost's type envelop (**I**), which corresponds to the stepwise mechanism (reactant -> **TS-I** -> **INT** -> **TS-I'** -> product), could be found.

When a metal cation (Li^+) was considered, three "folded-envelop" conformations could be located. These three TSs are the ones which have previously been suggested from the observed stereochemistry of the products. Figure 4 shows Trost's type **TS-I**, along with the intermediate (**INT**) and **TS-I'**. Figure 5 shows the transition structures corresponding to Rautenstrach's (**TS-II**) and Nakai's envelop (**TS-III**). The Li^+ bridges aldehyde moiety (C_1-O_2 part A, Figure 1) and allyl anion moiety (C_3-C_5, part B, Figure 1). The forming C_1-C_5 (2.198Å) and O_2-C_3 breaking bond length (1.537Å) indicates that **TS-I** corresponds to an early TS. The conformation around the forming C_1

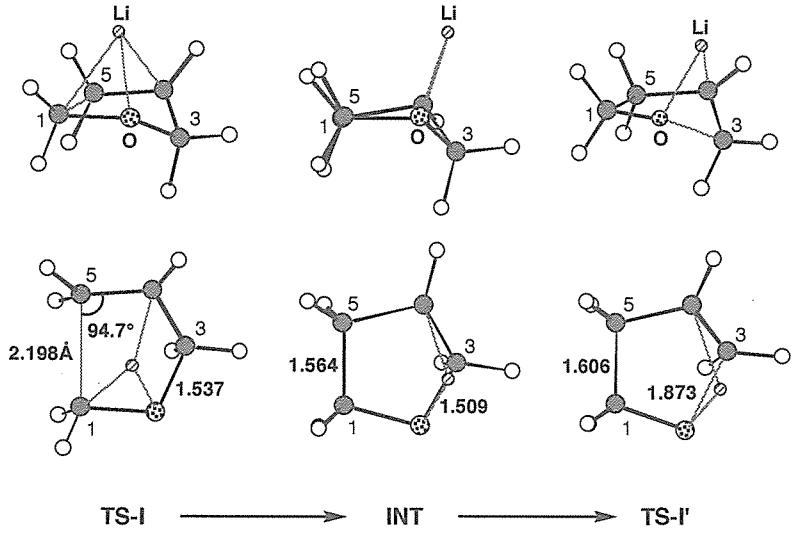

Figure 4. 3-21G transition structures (Trost's type (**TS-I** for C-C bond forming and **TS-I'** for C-O bond breaking step) and the intermediate (**INT**) for [2,3]-Wittig rearrangement of lithiated **1**.

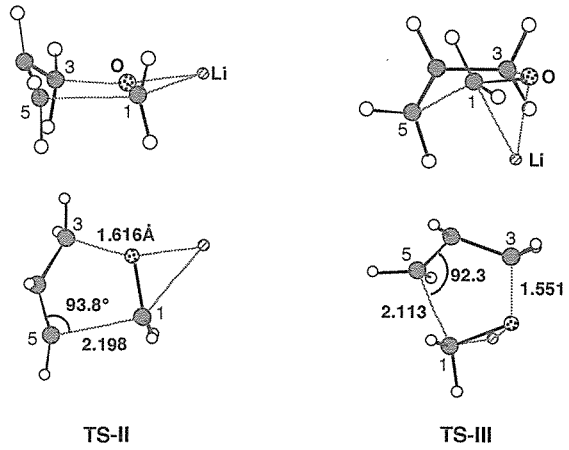

Figure 5. 3-21G transition structures (Rautenstrach's (**TS-II**) and Nakai's envelop (**TS-III**)) for [2,3]-Wittig rearrangement of lithiated **1**.

-C_5 bond is almost completely eclipsed (the dihedral angle O_2-C_1···C_5-C_4 is only 4.0°), in spite of the shorter distance (by 0.3Å between C_1 and C_5 atoms) and consequently the larger steric repulsion, as compared with the case of non-lithiated **TS-I** (Figure 3). This might be because of the remarkable stabilization of Trost's envelop by attractive coulomb interaction between Li cation and three negatively charged centers, namely, C_1, O_2, and growing anion at C_4. **TS-I'** also maintains complete eclipsed conformation around C_1-C_5 bond. Although non-lithiated and lithiated **TS-I's** have all fundamentally Trost's type envelop (**I**), the envelop lid is different (C_5) only for non-lithiated **TS-I'**, whereas C_3 is envelop lid for other three TSs. The O_2-C_3 atomic distance become smaller (1.873Å for lithiated **TS-I'** from 2.002Å for non-lithiated **TS-I'**), due to the coulomb attractive interaction between O_2, C_4, and bridging Li^+ connecting them.

TS-II has Rautenstrach's envelop conformation (**II**, Figure 2) with the partially formed C_1-C_5 bond nearly eclipsed with the partially broken C_3-O_2 bond (the dihedral angle C_3-O_2···C_1-C_5 is -2.9°). **TS-II** is the quite the same structure which Houk and Marshall et al. reported *ab initio* calculations of allyl lithiomethyl ether,[21] which is presented in Figure 5. It has been known that Rautenstrach's envelop corresponds to a concerted, thermally allowed sigmatropic process, which has the geometry corresponding to [2,3]-shift that proceeds in a suprafacial fashion with respect to two fragments, following the Woodward-Hoffmann rule[22] or the Fukui's frontier orbital theory.[23] Schematic representation of orbital interaction is also shown in Figure 1, in which the [2,3]-shift is a one-step S_Ni' reaction that proceeds in a suprafacial fashion with respect to both fragments as depicted in A and B. That is, it can be considered that two parts of the molecule, that is, the allyl and aldehyde anion fragments, interacts in the postulated five-center transition states. The forming C_1-C_5 and breaking O_2-C_3 bond length are 2.198 and 1.606Å, respectively, which shows that the O_2-C_3 bond breaking is more pronounced than Trost's **TS-I** (1.537Å) inspite of almost the same distance between C_1 and C_5 (2.198Å). Li cation locates on the extended line of O_2-C_3 breaking bond (the bond angle C_3. . . O_2. . . Li is 155.4°), which indicates that the O_2-C_3 bond breaking can be promoted more effectively than in **TS-I**. IRC calculation reveals that **TS-II** is corresponding to the concerted process, which directly

connects the reactant and the final alcohol without no intermediate. Lastly, **TS-III**, which has been originally proposed by Nakai et. al., has C_5 atom as envelop lid. Nakai's envelop (**III**) emphasizes the pseudo-1,3-diaxial interaction between C_1 and C_4 substituents and the gauche interaction between C_1 and C_5 substituents. **TS-III** has the shortest C_1-C_5 forming bond length (2.113Å) among the three TSs. The dihedral angle C_1-O_2..C_3-C_4 is only 0.6°. IRC calculation indicates that **TS-III** is also corresponding to concerted process.

Among these three transition structures, **TS-I** and **TS-III** belong to the "retention process", and **TS-II** to the "inversion process" of the lithio carbanion involved. In this point, the detailed discussion is to be reported.

Energies

Tables 1 and 2 collect the raw and relative energies for [2,3]-Wittig rearrangement of **1**, through **TS-I**, **TS-II**, and **TS-III**. Tables 1-1 and 1-2 present the raw and relative energies for the stepwise process through "non-lithiated" **TS-I**, **INT**, and **TS-I'**. Table 2 collects the raw energies for the "lithiated" **TS-I** for Table 2-1, **TS-II** and **TS-III** for Table 2-2, respectively. Table 2-3 shows the relative energies for the path through lithiated **TS-I**, **INT**, and **TS-I'**. Table 2-4 shows the summarized activation enthalpies ($\Delta H^{\neq}$) of **TS-II** and **TS-III**, along with **TS-I**.

The MP2/6-31(+)G(*) energy calculation at 3-21G optimized geometries for non-lithiated **1** are

Table 1-1. The energies (a.u., //3-21G) for [2,3]-Wittig rearrangement of non-lithiated **1**.

calcn. level	Reactant	**TS-I**	**INT**	**TS-II**	Product
3-21G	−228.957542	−228.934728	−228.991404	−228.983910	−229.014213
6-31G	−230.143153	−230.118385	**−230.170831**	**−230.175289**	−230.223459
6-31G*	−230.235069	−230.206732	−230.269968	−230.262239	−230.312071
6-31+G	−230.172407	−230.146313	**−230.195803**	**−230.200246**	−230.250515
6-31+G*	−230.264656	−230.235506	−230.295246	−230.288775	−230.340606
MP2/6-31G	−230.621646	−230.615524	**−230.652715**	**−230.680174**	−230.708782
MP2/6-31G*	−230.928339	−230.922174	**−230.972339**	**−230.986389**	−231.012393
MP2/6-31+G	−230.672143	−230.664794	**−230.700966**	**−230.725957**	−230.757405
MP2/6-31+G*	−230.977030	−230.970420	**−231.017981**	**−231.031587**	−231.060197

Table 1-2. Relative energies (kcal/mol, //3-21G) for [2,3]-Wittig rearrangement of non-lithiated **1**.

calcn. level	$\Delta H_{TS-I}^{\neq}$	$\Delta H_{TS-I'}^{\neq}$	$\Delta H(H_{TS-I}-H_{TS-I'})$	ΔH_0
3-21G	14.3	4.7	−30.9	−35.6
6-31G	15.5	—	−35.7	−50.4
6-31G*	17.8	4.9	−34.8	−48.3
6-31+G	16.4	—	−33.8	−49.0
6-31+G*	18.3	—	−33.4	−47.7
MP2/6-31G	3.8	—	−40.6	−54.7
MP2/6-31G*	3.9	—	−40.3	−52.7
MP2/6-31+G	4.6	—	−38.4	−53.5
MP2/6-31+G*	4.1	—	−38.4	−52.2

very problematical. Table 1-1 reveals that the raw energies of the intermediate (**INT**) and the transition structure (**TS-I'**) are reversed, except those at RHF/3-21G//3-21G and RHF/6-31G*//3-21G levels. That is, the energies of **INT** are higher than those of **TS-I'**. This result indicates that the consideration of counterion (Li^+) is important to evaluate the energy differences between the stationary points. Certainly, as shown in Table 2-1, the differences in energies for lithiated species are satisfactory to describe the reaction paths of [2,3]-Wittig rearrangement. The activation enthalpies ($\Delta H^{\neq}$) for non-lithiated **TS-I**, obtained at 3-21G optimized structures, are calculated to be 14~19 kcal/mol at RHF level and these values remarkably decreases to only 3-4 kcal/mol at MP2

Table 2-1. The energies (Trost's envelops (**TS-I** and **TS-I'**, a.u., //3-21G) for [2,3]-Wittig rearrangement of lithiated **1**.

calcn. level	Reactant	**TS-I**	**INT**	**TS-I'**	Product[a)]
3-21G	−236.477744	−236.422465	−236.494011	−236.466998	−236.542743 (−236.547458)
6-31G	−237.695193	−237.628571	−237.699317	−237.678409	−237.770101 (−237.771746)
6-31G*	−237.777214	−237.719956	−237.794397	−237.762829	−237.848992 (−237.856032)
6-31+G	−237.705480	−237.635815	−237.704896	−237.685548	−237.782115 (−237.780386)
6-31+G*	−237.786446	−237.726731	−237.799100	−237.769816	−237.860168 (−237.864458)
MP2/6-31G	−238.175860	−238.136725	−238.190026	−238.183560	−238.256356 (−238.258654)
MP2/6-31G*	−238.478192	−238.455170	−238.509870	−238.493792	−238.554835 (−238.564254)
MP2/6-31+G	−238.195068	−238.153324	−238.204236	−238.200229	−238.276709 (−238.275950)
MP2/6-31+G*	−238.495664	−238.470686	−238.522600	−238.509542	−238.573266 (−238.580240)

a) The energies for product having linear geometry are also shown in parenthesis.

Table 2-2. The energies (Rautenstrach's (**TS-II**) and Nakai's envelop (**TS-III**), a.u., //3-21G) for [2,3]-Wittig rearrangement of lithiated **1**.

calcn. level	**TS-II**	**TS-III**
3-21G	−236.411142	−236.394083
6-31G	−237.621950	−237.600712
6-31G*	−237.698852	−237.690738
6-31+G	−237.634221	−237.611540
6-31+G*	−237.710726	−237.700834
MP2/6-31G	−238.132557	−238.110396
MP2/6-31G*	−238.439171	−238.425602
MP2/6-31+G	−238.155222	−238.131474
MP2/6-31+G*	−238.459495	−238.444735

Table 2-3. Relative energies (kcal/mol, //3-21G) of path **I** (proceeding through Trost's envelops (**TS-I** and **TS-I'**)) for [2,3]-Wittig rearrangement of lithiated **1**.

calcn. level	$\Delta H_{TS-I}^{\neq}$	$\Delta H_{TS-I'}^{\neq}$	$\Delta H(H_{TS-I}-H_{TS-I'})$	ΔH_0
3-21G	34.7	17.0	−27.9	−40.8
6-31G	41.8	13.1	−31.3	−47.0
6-31G*	35.9	19.8	−26.9	−45.0
6-31+G	43.7	12.1	−31.2	−48.1
6-31+G*	37.5	18.4	−27.0	−46.3
MP2/6-31G	24.6	4.1	−29.4	−50.5
MP2/6-31G*	14.4	10.1	−24.2	−48.1
MP2/6-31+G	26.2	2.5	−29.4	−51.2
MP2/6-31+G*	15.7	8.2	−24.4	−48.7

Table 2-4. Activation enthalpies (kcal/mol, //3-21G) of **TS-I**, **TS-II**, and **TS-III** for [2,3]-Wittig rearrangement of lithiated **1**.

calcn. level	$\Delta H_{TS-I}^{\neq}$	$\Delta H_{TS-II}^{\neq}$	$\Delta H_{TS-III}^{\neq}$
3-21G	34.7	41.8	52.5
6-31G	41.8	46.0	59.3
6-31G*	35.9	49.2	54.3
6-31+G	43.7	44.7	58.9
6-31+G*	37.5	47.5	53.7
MP2/6-31G	24.6	27.2	41.1
MP2/6-31G*	14.4	24.5	33.0
MP2/6-31+G	26.2	25.0	39.9
MP2/6-31+G*	15.7	22.7	32.0

level. On the other hand, for lithiated **TS-I**, $\Delta H^{\neq}$ values were calculated to be 34~44 kcal/mol at RHF level, which are quite larger than those of non-lithiated species. (Table 1-2 vs. Table 2-3) These $\Delta H^{\neq}$ values become much smaller (14~26 kcal/mol) at MP2/6-31(+)G(*) levels, which are reasonable values, as compared with experimental conditions. The transition structures (**TS-I'**), in which O_2-C_3 bond cleavage occurs, are much stable (by 20~30 kcal/mol) than **TS-I**, indicating that C-C bond forming **TS-I** is the rate determining step. The $\Delta H^{\neq}$ values for **TS-I'** (the energy difference between **INT** and **TS-I'**) are smaller (2~10 kcal/mol at MP2 level) than those (14~27 kcal/mol) between the reactants and **TS-I**. The reaction is calculated to be very exothermic (ΔH_0=−40~−50 kcal/mol), as shown in Table 2-3. Finally, Table 2-4 presents $\Delta H^{\neq}$ values for three paths proceeding through lithiated **TS-I**, **TS-II**, and **TS-III**. Interestingly, **TS-I**, which is corresponding to the stepwise mechanism, is more stable than the concerted **TS-II** and **TS-III** at all levels except MP2/6-31+G level, suggesting that the route of stepwise mechanism (eq.3, Figure 1) can not be excluded. **TS-III** is the most unstable (by at least 13 kcal/mol as compared with those of **TS-I**). Thus, the energetic consideration shows that the activation enthalpies are the smallest for stepwise **TS-I**, and **TS-III** is the most highest. Of course, these energy differences calculated in this study might change considerably for the reaction of substituted **1**. The transition structures and energies for [2,3]-Wittig

rearrangement of substituted **1** are to be published.

The basis set dependency for activation enthalpy are obvious. As shown in Table 2-4, $\Delta H^{\neq}$ values at MP2/6-31(+)G level for **TS-I** and **TS-II** are very close, though the differences between the energies estimated at MP2/6-31G* and MP2/6-31+G* levels are quite large (7~10 kcal/mol). This tendency indicates that the polarization function (*) seems to understimate (by ~10 kcal/mol) the $\Delta H^{\neq}$ of **TS-I**, since $\Delta H^{\neq}$ of **TS-II** are unchanged (22~27 kcal/mol) at all MP2/6-31(+)G(*) levels. The same trend was found for **TS-III**.

Potential Energy Profiles along the IRC

Next, IRC calculations were performed for **TS-I** and **TS-II** to clarify whether TS geometries connect the reactants and the products. Figures 6 and 7 display the potential energy profiles of the reaction paths proceeding through **TS-I** and **TS-II** along the IRC, respectively, where s=0.0 $amu^{1/2}$

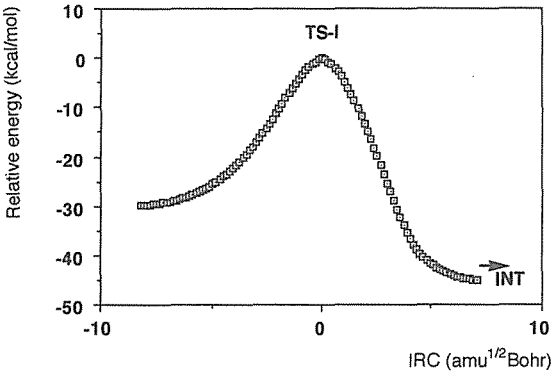

Figure 6-1. Potential energy profile along the IRC (intrinsic reaction coordinate) for stepwise path proceeding through Trost's envelop (**TS-I**), leading to the five-membered intermediate (**INT**).

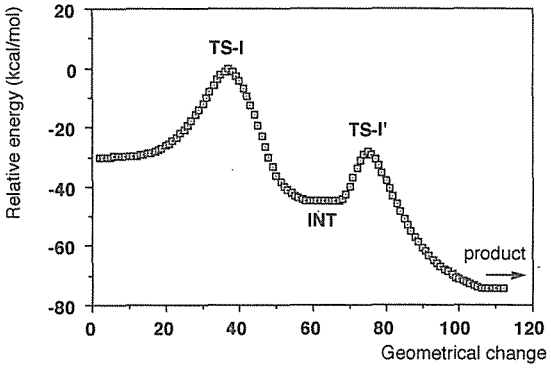

Figure 6-2. Potential energy profile along the IRC (intrinsic reaction coordinate) for stepwise path proceeding through Trost's envelop (**TS-I**), the five-membered intermediate (**INT**), and **TS-I'**.

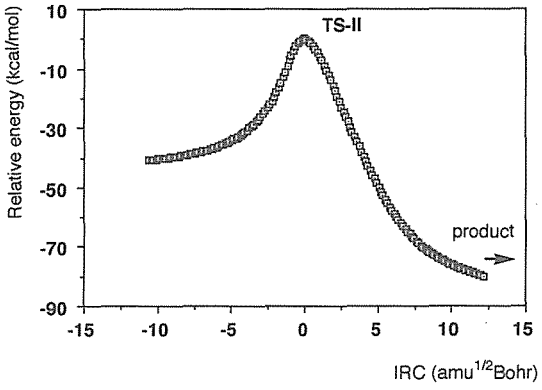

Figure 7. Potential energy profile along the IRC (intrinsic reaction coordinate) for concerted path proceeding through Rautenstrach's envelop (**TS-II**).

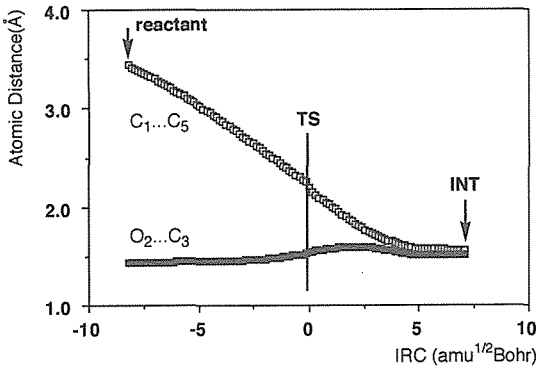

Figure 8. The change of $C_1 \ldots C_5$ and $O_2 \ldots C_3$ atomic distances along the IRC of stepwise path (proceeding through Trost's envelop (**TS-I**), leading to **INT**).

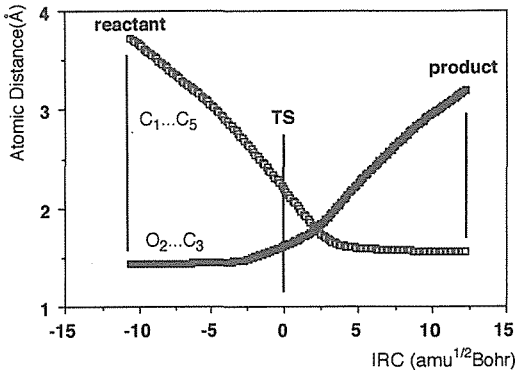

Figure 9. The chamge of $C_1 \ldots C_5$ and $O_2 \ldots C_3$ atomic distances along the IRC of concerted path (proceeding through Rautenstrach's envelop (**TS-II**)).

Bohr stands for the TS. For **TS-I**, Figures 6-1 and 6-2 show the potential energy profile for C_1-C_5 bond forming **TS-I** giving **INT**, and that including O_2-C_3 bond breaking **TS-I'** which gives the final alcohol, respectively. Attractive coulomb interaction between Li^+ and the three anion centers considerably stabilized five-membered **INT**, and therefore, the reaction become stepwise. In other words, although Li^+ can effectively stabilize the growing negative charge on C_4 atom, this interaction prevents the separation of aldehyde (C_1-O_2) and allyl anion moiety (C_3-C_5). This interaction does not exist in **TS-II** and **TS-III** for concerted processes. **TS-II** connects the reactant and the alcoholic product directly (concerted process), without the intervention of the intermediate, as shown in Figure 7. Thus, it could be clarified from the calculations that attractive coulomb interaction between Li^+ and growing C_4 anion centers plays a major role in facilitating the formation of the five-membered intermediate and in making the path proceeding **TS-I** stepwise.

Geometry transformation along the IRC

Figures 8 and 9 display the relationship between the forming C_1-C_5 and breaking O_2-C_3 bond lengths for **TS-I** and **TS-II** along the IRC, respectively. The curves for **TS-I** (Figure 8) shows that the distance between C_1 and C_5 atoms monotonously shortened, though that between O_2 and C_3 atoms was unchanged. After the TS, O_2-C_3 bond is elongated slightly (1.537Å for TS to 1.592Å (s=2.10)). This fact indicates that there still have some concerted nature for C-C bond forming and O-C bond breaking occur cooperatively. However, the driving force for O_2-C_3 bond breaking is too weak as compared with the O_2—Li—C_4 attractive coulomb interaction. Figure 9 shows the very different curves with those in Figure 8 (for **TS-I**). The O_2-C_3 bond is lengthened rapidly after the TS, which indicates the C_1-C_5 bond forming and O_2-C_3 bond breaking occur concertedly. This concerted nature can be ascribed to the position of Li atom. In **TS-II**, Li^+ locates at the extension of the breaking O_2-C_3 bond. The bond angle of Li^+-O_2-C_3 is 155.4° in **TS-II**, indicating that the positive charge of Li^+ can attract the growing anion at O_2 effectively and consequently promote to separate O_2 atom from C_3. Moreover, Li^+, located at the opposite side with C_3, does not fasten C_1-O_2 moiety to allyl anion

moiety but helps product development, whereas the bridging of Li^+ between two moieties makes **TS-I** stepwise and leads to five-membered **INT**.

Finally, Figures 10 and 11 displays the geometry transformations for **TS-I** and **TS-II** along the IRC, respectively. Figure 10-1, 10-2 and 11-1, 11-2 are the front and side views for **TS-I** and **TS-II**, respectively. The most different point between these two modes is the nature of attacking anionic lobes. In **TS-I** (Figure 11), C_1 atom attacks to C_5 by using front lobe (retention process, Li and C_5 atoms locate on the same side with respect to the average plane of HC_1H-O_2 moiety), whereas in **TS-II** (Figure 12), C_1 attacks to C_5 by using back lobe (inversion process, Li and C_5 atoms locate on the opposite side).

Summary

This computational study for [2, 3]-Wittig rearrangement could clarify the following points:

(1) Transition structures (TS-I, TS-II, and TS-III) for the reaction of allyloxymethyllithium (1) have been located at the 3-21G basis set, whereas only one transition structure was found for the reaction of its anionic species.

(2) TS-I is the transition structure leading to 5-membered ring intermediate (INT), followed by O_2-C_3 bond breaking TS-I' (stepwise pathway). TS-II and TS-III are the ones for the concerted pathway, in which C_1-C_5 bond forming and O_2-C_3 bond breaking occurred simultaneously.

(3) TS-III is the most unstable transition structure among the three transition structures and TS-I and TS-II have almost the same activation enthalpies, though the energies remarkably depend on the calculation levels.

(4) In TS-I, the coulomb attractive interaction of O_2... Li...C_4 impedes the separation of O_2 and C_3 atoms (therefore, the O_2-C_3 bond breaking become difficult). On the other hand, TS-II and TS-III, in which Li interacts strongly only with O_2 atom, is the one corresponding to the concerted pathway because that the growing negative charge on O_2 by O_2-C_3 bond breaking can be stabilized effectively with Li atom.

Acknowledgment

The author thanks to Saga University Information Processing Center, for the use of Power Indigo 2 work station.

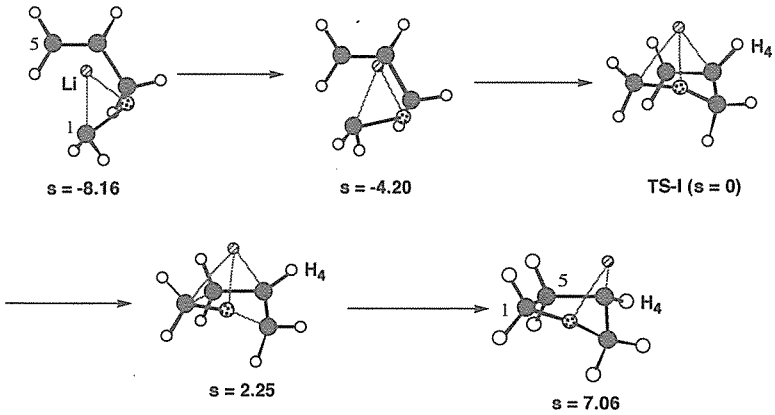

Figure 10-1. Geometrical change along the IRC for the path proceeding through **TS-I** at the 3-21G basis set. Values under each geometries indicate the lengths from the transition structure in amu$^{1/2}$ Bohr unit.

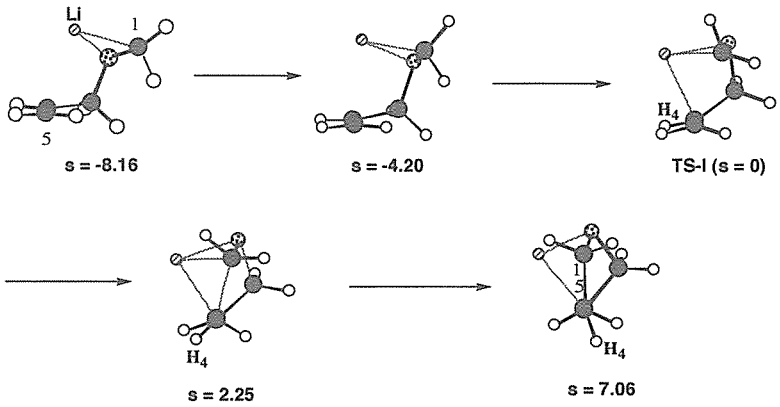

Figure 10-2. Side view of geometrical change along the IRC for the path proceeding through **TS-I** at the 3-21G basis set. Values under each geometries indicate the lengths from the transition structure in amu$^{1/2}$ Bohr unit.

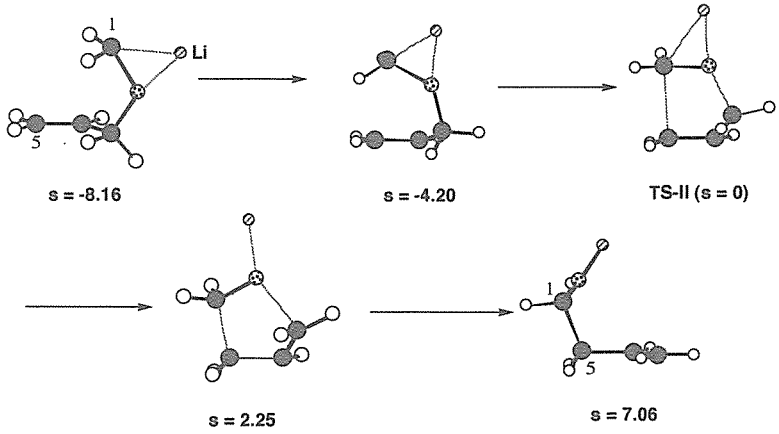

Figure 11-1. Front view of geometrical change along the IRC for the path proceeding through **TS-II** at the 3-21G basis set. Values under each geometries indicate the lengths from the transition structure in amu$^{1/2}$ Bohr unit.

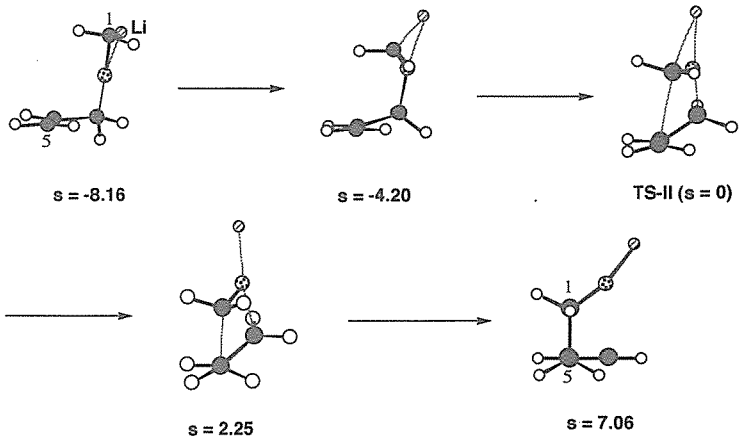

Figure 11-2. Side view of geometrical change along the IRC for the path proceeding through **TS-II** at the 3-21G basis set. Values under each geometries indicate the lengths from the transition structure in amu$^{1/2}$ Bohr unit.

References and Notes

1. (a) Jefferson, A.; Scheinmann, F. Quart. Rev. **1968**, 22, 391. (b) Hansen, H.-J.; Sutter, B.; Schmid, H. *Helv. Chim. Acta* **1968**, 51, 828. (c) Scholosser, M. *J. Organometallic Chem.* **1967**, 8, 9. (d) Schollkopf, U.; Fellenberger, K. *Annalen,* **1966**, 698, 80. (e) Makisumi, Y.; Notzumoto, S. *TetrahedronLett.* **1966**, 6393. (f) Hauser, C. R.; Kantor, S. W. *J. Am. Chem. Soc.* **1951**, 73, 1437.
2. For reviews on stereoselective synthesis of acyclic compounds, see: (a) Masamune, S.; Choy, W. *Aldrichimica Acta* **1982**, 15, 47. (b) Evans, D. A.; Nelson, J. V.; Taber, T. R. In *Top. Stereochem.* **1982**, 13, 1. (c) Hoffmann, R. W. *Angew. Chem., Int. Ed. Engl.* **1982**, 21, 555. (d) Heathcock, C. H. *Science* (Washingtoc, D.C.) **1981**, 214, 395. (e) Bartlett, P. A. *Tetrahedron,* **1980**, 36, 3.
3. For a review on [2,3] sigmatropic rearrangements, see: (a) Mikami, K.; Nakai, T. *Synthesis* **1991**, 594. Marshall, "Comprehensive Organic Synthesis," ed by Trost, B. M. and Fleming, I., Pregamon Press, London (1991), Vol.3, pp.975. (b) Nakai, T.; K. *Chem. Rev.* **1986**, 86, 885. (c) Hill, R. K, "Chirality Transfer via Sigmatropic Rearrangements," in: "Asymmetric Synthesis," Morrison, J. D. (Ed.), Vol.3, Chapter 8, Academic Press, Inc. 1984, 503. (d) Vedejs, E. *Acc. Chem. Res.* **1984**, 17, 358. (e) Nakai, T.; Mikami, K.; Sayo, N. *J. Synth. Org. Chem., Jpn.* **1983**, 41, 100. (f) Hoffmann, R. W. *Angew. Chem.* **1979**, 91, 625. (g) Hoffmann, R. W. *Angew. Chem., Int. Ed. Engl.* **1979**, 18, 563. (h) Still, W. C.; Mitra, A. *J. Am. Chem. Soc.* **1978**, 100, 1927. (i) Chan, K.; Saucy, G. *J. Org. Chem.* **1977**, 42, 3828. (j) Baldwin, J. E.; Patrick, J. E. *J. Am. Chem. Soc.* **1971**, 93, 3556.
4. (a) Bond, D.; Schleyer, P. v. R. *J. Org. Chem.* **1990**, 55, 1003. (b) Broka, C. A. Hu, L.; Lee, W. J.; Shen, T. *TetrahedronLett.* **1987**, 28, 4993. (c) Kano, S.; Yokomatsu, T.; Nemoto, H.; Shibuya, S. *J. Am. Chem. Soc.* **1986**, 108, 6746. (d) Oppolzer, W.; Stevenson, T. *TetrahedronLett.* **1986**, 27, 1139. (e) Marshall, J. A.; Jenson, T. M. *J. Org. Chem.* **1984**, 49, 1707. (f) Sayo, N.; Kitahara, E.; Nakai, T. *Chem. Lett.* **1984**, 259. (g) Nakai, T.; Mikami, K.; Taya, S.; Kimura, Y.; Mimura, T. *TetrahedronLett.* **1981**, 22, 69. (h) Still, W. C.; McDonald III, J. H.; Collum, D. B.; Mitra, A. *TetrahedronLett.* **1979**, 593. (i) Still, W. C.; Mitra, A. *J. Am. Chem. Soc.* **1978**, 100, 1927. (j) Schleyer, P. v. R.; Dill, J. D.; Pople, J. A.; Hehre, W. J. *Tetrahedron* **1977**, 33, 2497. (k) Schlosser, M.; Hartmann, J. *J. Am. Chem. Soc.* **1976**, 98, 4674.
5. For [2,3]-Wittig rearrahgement of sulfur ylide, see: (a) Vedejs, E.; Buchanan, R. A.; Conrad, P. C.; Meier, G. P.; Mullins, M. J.; Schaffhausen, J. G.; Schwartz, C. E. *J. Am. Chem. Soc.* **1989**, 111, 8421. (b) Yedejs, E.; Buchanan, R. A.; Conrad, P. C.; Meier, G. P.; Mullins, M. J.; Watanabe, Y. *J. Am. Chem. Soc.* **1987**, 109, 5878. (c) Vedejs, E.; Buchana, R. A. *J. Org. Chem.* **1984**, 49, 1840. (d) Vedejs, E. *Acc. Chem.*

Res. **1984**, 17, 358. (e) Vedejs, E.; Powell, D. W. *J. Am. Chem. Soc.* **1982**, 104, 2046. (f) Cere, V.; Paolucci, C.; Pollicino, S.; Sandri, E.; Fava, A. *J. Org. Chem.* **1979**, 44, 4128; *Ibid.* **1981**, 46, 3315. (g) Fava, A.; Paolucci, C.; Policino, S.; Sandri, E. *J. Org. Chem.* **1978**, 43, 4826. (h) Vedejs, E.; Mullins, M.; Renga, J. M.; Singer, S. P. *TetrahedronLett.* **1978**, 519. (i) Vedejs, E.; Hegan, J. P.; Roach, B. L.; Spear, K. L. *J. Org. Chem.* **1978**, 43, 1185. (j) Vedejs, E.; Arco, M. J.; Powell, D. W.; Renga, J. M.; Singer, S. P. *J. Org. Chem.* **1978**, 43, 4831. (k) Vedejs, E.; Hagen, J. P. *J. Am. Chem. Soc.* **1975**, 97, 6878.

6. Kruse, B.; Bruckner, R, *TetrahedronLett.* **1990**, 31, 4425.
7. (a) Jamison, R. W.; Laird, T.; Ollis, W. D.; Sutherland, I. O. *J. Chem. Soc., Perkin Trans. I* **1980**, 1436. (b) Trost, B. M.; Melvin, L. S., Jr. *Sulfur Ylides*; Academic Press: New York, 1975; Chapter 7. (c) Evans, D. A.; Angews, G. C. *Acc. Chem. Res.* **1974**, 7, 147. (d) Baldwin, J. E.; Hackler, R. E.; Kelly, D. P. *J. Chem. Soc., Chem. Commun.* **1968**, 538.
8. Trost, B. M.; Melvin, L. S., Jr. *Sulfur Ylides*; Academic Press: New York, 1975; Chapter 7.
9. (a) Rautenstrach, V. *J. Chem. Soc., Chem. Commun.* **1970**, 4. (b) Wu, Y-D.; Houk, K. N. *J. Org. Chem.* **1991**, 56, 5657. (c) Wu, Y.-D.; Houk, K. N.; Masshall, J. A. *J. Org. Chem.* **1990**, 55, 1421. (d) Kruse, B.; Bruckner, R. *TetrahedronLett.* **1990**, 31, 4425. (e) Midland, M. M.; Gabriel, J. *J. Org. Chem.* **1985**, 50, 1143. (f) Midland, M. M.; Kwon, Y. C. *TetrahedronLett.* **1985**, 26, 5013. (g) Tsai, D. J-S.; Midland, M. M. *J. Org. Chem.* **1984**, 49, 1842.
10. (a) Fujimoto, K.; Sakai, H.; Nakai, T. *Chem Lett.* **1933**, 1397. Nakai, E.; Nakai, T. *TetrahedronLett.* **1988**, 29, 5409. (b) Mikami, K.; Nakai, T. *Physical Organic Chemistry*; Kobayashi, M. Ed.; vol.31, Elsevier: Amsterdam, **1987**, pp.153. (c) Takahashi, O.; Saka, T.; Mikami, K.; Nakai, T. *Chem. Lett.* **1986**, 1599. Kasuga, T.; Nakai, T.; *Chem. Lett.* **1985**, 1729. (d) Sayo, N.; Azuma, K.; Mikami, K.; Nakai, T. *TetrahedronLett.* **1984**, 25, 565. (e) Mikami, K.; Azuma, K.; Nakai, T. *Tetrahedron* **1984**, 16, 2303. (f) Mikami, K.; Azuma, K.; Nakai, T. *Tetrahedron* **1984**, 40, 2303. (g) Mikami, K.; Kimura, Y.; Kishi, N.; Nakai, T. *J. Org. Chem.* **1983**, 48, 279. (h) Mikami, K.; Kimura, Y.; Kishi, N.; Nakai, T. *J. Org. Chem.* **1983**, 48, 279. (i) Mikami, K.; Fujimoto, K.; Nakai, T. *TetrahedronLett.* **1983**, 24, 513. (j) Sayo, N.; Kimura, Y.; Nakai, T. *TetrahedronLett.* **1982**, 23, 3931. (k) Nakai, T.; Mikami, T.; Taya, S.; Fujita, Y. *J. Am. Chem. Soc.* **1981**, 103, 6492.
11. Takahashi, T.; Nemoto, H.; Kanda, Y.; Tsuji, J.; Fukazawa, Y.; Okajima, T.; Fujise, Y. *Tetrahedron* **1987**, 43, 5499.
12. Hehre, W. J.; Radom, L.; Schleyer, P. v. R.; Pople, J. A. *Ab initio Molecular Orbital Theory*; John Wiley and Sons: New York, 1986; (a) pp466-504. (b) pp96
13. Baker, J. *J. Comput. Chem.* **1986**, 7, 385.
14. (a) Hobza, P.; Zahradnik, R. *Chem. Rev.* **1988**, 88, 871; Kaufmann, E.; Schleyer, P. v. R.; Houk, K. N.; Y -D. J. *Amer. Chem. Soc.*, **1985**, 107, 5560.
15. Spitznagel, G. W.; Clark, T.; Chandrasekhar, J.; Schleyer, P. v. R. *J. Comput. Chem.* 1982, **3**, 363: 3-21G; Gordon, M. S.; Binkley, J. S.; Pople, J. A.; Pietro, W. J.; Hehre, W. J. *J. Amer. Chem. Soc.* **1982**, 104, 2797; Binhley, J. S.; Pople, J. A.; Hehre, W. J. *J. Amer. Chem. Soc.* **1980**, 102, 939; Dobbs, K. D.; Hehre, W. J. *J. Comput. Chem.* **1986**, 7, 359;
6-31G*; Hariharan, P. C.; Pople, J. A.; *Chem. Phys. Lett.* **1972**, 16, 217; Hariharan, P. C. Pople, J. A. *Theor. Chim Acta* **1973**, 28, 213; Hariharan, P. C.; Pople, J. A. *Mol. Phys.* **1974**, 27, 209; Dill, J. D.; Pople, J. A. *J. Chem. Phys.* **1975**, 62, 2921; Francl, M. M.; Pietro, W. J.; Hehre, W. J.; Gordon, M. S.; Defrees, D. J.; Pople, J. A. *J. Chem. Phys.* **1982**, 77, 3654;
6-31+G*, Clark, T.; Chandrasekhar, J.; Spitznagel, G.; Schleyer, P. v. R. *J. Comp. Chem.* **1983**, 4, 294.
16. Moller, C.; Plesset, M. S. *Phys. R.* **1934**, 46, 618; Krishman, R.; Krishman, R.; Frish, M. J.; Pople, J. A. *J. Chem. Phys.* **1980**, 72, 4244; Pople, J. A. *Int. J. Quant. Chem. Symp.* **1978**, 14, 91; Pople, J. A.; Seeger, R.; Krishman, R. *Int. J. Quant. Chem. Symp.* **1977**, 11, 49; Pople, J. A.; Binkley, J. S.; Seeger, R. *Int. J. Quantum. Chem. Symp.* **1976**, 10, 1:
17. Abbreviation "MPs" generally means the n-th order Moller-Plesset perturbational method.

18. Ragavachari, K.; Frisch, M. J.; Pople, J. A. *Int. J. Quant. Chem.* **1978**, 14, 91.
19. Hehre, W. J.; Radom, L.; Schleyer, P. v. R.; Pople, J. A. *Ab initio Molecular Orbital Theory*; Wiley & Sons Inc.: New York, 1986; pp310-321.
20. Houk, K. N.; Li, Y.; Evanseck, J. D. *Angew. Chem. Int. Ed. Engl.* **1992**, 31, 682.
21. Wu, Y.-D.; Houk, K. N.; Marshall, J. A. *J. Org. Chem.* **1990**, 55, 1421.
22. Woodward, R. B.; Hoffmann, R. *The Conservation of Orbital Symmetry; Academic:* New York, 1970.
23. (a) Fukui, K. *Theory of Orientation and Stereoselection*; Springer-Verlag: Berlin, 1971. (b) Fleming, I. *Frontier Orbitals and Organic Chemical reactions*; Wiley: New York, 1976.